Engineering Fracture Mechanics 77 (2010) 2567–2576

Contents lists available at ScienceDirect

Engineering Fracture Mechanics

journal homepage: www.elsevier.com/locate/engfracmech

# Numerical analysis on special cracking phenomena of residual compressive inter-layers in ceramic laminates

C.R. Chen [a,d,e,*], R. Bermejo [b], O. Kolednik [c]

[a] Materials Center Leoben, A-8700 Leoben, Austria
[b] Institut für Struktur- und Funktionskeramik, Montanuniversität Leoben, A-8700 Leoben, Austria
[c] Erich Schmid Institute of Materials Science, Austrian Academy of Sciences, A-8700 Leoben, Austria
[d] Centre for Advanced Materials Technology (CAMT), School of Aerospace, Mechanical and Mechatronic Engineering, University of Sydney, Australia
[e] State Key Lab of Metal Matrix Composites, Shanghai Jiao Tong University, Shanghai 200240, China

ARTICLE INFO

*Article history:*
Received 2 November 2009
Received in revised form 26 May 2010
Accepted 21 June 2010
Available online 25 June 2010

*Keywords:*
Residual stress
Layered ceramics
Finite element analysis
*J*-integral
Brittle fracture

ABSTRACT

Finite element computations are performed to analyze the phenomena of edge cracking and crack bifurcation in two ceramic laminates composed by tensile thick layers and compressive thin layers. The difference between these two laminates is the thickness of the compressive thin layers. Experimental results performed by one of the authors in previous works show that edge cracks exist in only one laminate, while crack bifurcation occurs in both laminates under bending. To understand the cracking phenomena observed in experiments, the energy release rates are calculated. Numerical results show that the initiation of crack bifurcation can be explained by the near-tip *J*-integral, provided that micro-cracks exist near the crack tip.



## 1. Introduction

### 1.1. Layered ceramics with residual stresses

Layered ceramic composites have been proposed as an alternative design to enhance the strength reliability of ceramic components as well as to improve their fracture toughness by means of energy release mechanisms, such as crack deflection or crack bifurcation [1–3]. A direct consequence of these energy-dissipation toughening mechanisms which reduce the crack driving force at the crack tip is the development of an increasing crack growth resistance, i.e., *R*-curve behaviour. Ceramics that exhibit this behaviour can reduce the scatter in fracture strength. A commonly used design of layered ceramics is to combine layers with differential thermal strain during cooling from the sintering temperature, yielding a tensile-compressive residual stress distribution. The specific location of the compressive layers, either at the surface or internal, is associated with the attempted design approach, based on either mechanical resistance or damage tolerance [4]. Compressive stresses can enhance the mechanical properties of the material, while tensile residual stresses can lead to crack formation (e.g., tunneling cracks, edge cracks) which may affect the structural integrity of the material.

* Corresponding author at: State Key Lab of Metal Matrix Composites, Shanghai Jiao Tong University, Shanghai 200240, China. Tel.: +86 13761742152; fax: +86 21 34202749.
*E-mail address:* crchen64@yahoo.com.cn (C.R. Chen).

0013-7944/$ - see front matter © 2010 Elsevier Ltd. All rights reserved.
doi:10.1016/j.engfracmech.2010.06.020

**Nomenclature**

| | |
|---|---|
| $a$ | depth of surface crack or edge crack |
| $a_L$ | half length of surface crack |
| $b$ | length of crack normal to interface under bending |
| $c$ | branch length of bifurcated crack |
| $G$ | elastic strain energy release rate |
| $G_{CH}$ | elastic strain energy release rate for channelling |
| $G_{ED}$ | elastic strain energy release rate for edging |
| $J_{Ic}$ | critical $J$-integral |
| $J_{tip}$ | crack tip $J$-integral |
| $K_{Ic}$ | critical stress intensity factor |
| $t_1$ | thickness of ATZ thick layer |
| $t_2$ | thickness of AMZ thin layer |
| $t_c$ | critical thickness of AMZ layer below which edge cracking cannot occur |
| $\Delta\varepsilon$ | strain difference between AMZ and ATZ layers at room temperature |
| $\sigma_R$ | planar residual stress in the compressive layer |
| $\sigma_m$ | stress at the upper surface of the specimen, caused by applied load |
| $\sigma_m^{crit}$ | critical value of $\sigma_m$ that makes $J_{tip} = J_{Ic}$ |
| $\sigma_m^f$ | $\sigma_m$ value corresponding to specimen failure |
| $\sigma_1$ | planar residual stress in the tensile ATZ layer |
| $\sigma_2$ | planar residual stress in the compressive AMZ layer |
| ATZ | $Al_2O_3$/5 vol.% t-$ZrO_2$ |
| AMZ | $Al_2O_3$/30 vol.% m-$ZrO_2$ |

### 1.2. Edge cracking of a compressive layer between tensile layers

The residual stress state near the edge surfaces of a laminate is different from that within the laminate. In the region far from the edge surfaces, biaxial residual stresses parallel to the layer plane exist, and the stress perpendicular to the layer plane is zero. Near the edge surfaces, however, the stress state is not biaxial since the edge surface is traction-free. As a result, a stress component perpendicular to the layer plane appears at the edge surface. The sign of this stress is opposite to that of the biaxial stresses in the interior. For a compressive thin layer between two tensile thick layers, a tensile residual stress perpendicular to the layer plane exists near the edge surface. This tensile residual stress decreases rapidly from the edge surface to become negligible at a distance of about the layer thickness [5–8]. The tensile residual stress near the edge surface may create "edge cracks" from pre-existing flaws. An edge crack propagates in two directions (Fig. 1): along the mid-line of the edge surface ("channelling") and along the direction normal to the edge surface into the interior of the layer ("edging"). A critical thickness $t_c$ exists for the compressive layer, below which channelling cannot occur regardless of the flaw size [5]:

$$t_c = \frac{K_{Ic}^2}{0.34\sigma_R^2}. \tag{1}$$

$K_{Ic}$ and $\sigma_R$ denote the critical stress intensity factor and the planar residual stress of the compressive layer, respectively. Eq. (1) is derived by setting the maximum strain energy release rate for channelling equal to the critical fracture energy of the compressive layer, assuming that the tensile layer thickness is much larger than the compressive layer thickness and that no

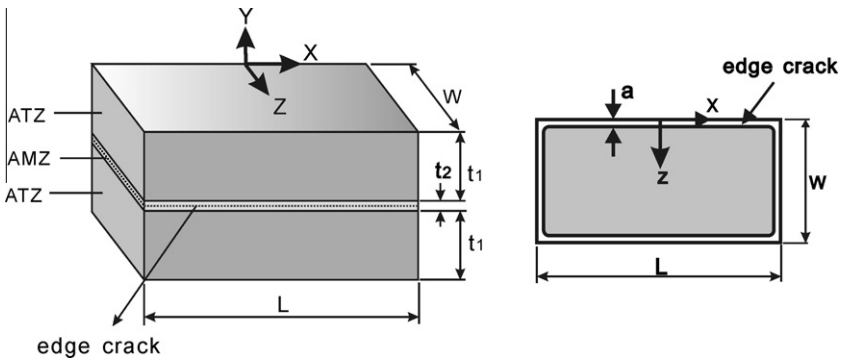


**Fig. 1.** Schematic of an edge crack along the mid-line of the surfaces of a compressive layer.

elastic mismatch exists. Experimental results show that edge cracking occurs in the laminates with the compressive layer thickness exceeding $2t_c$ [8].

### 1.3. Crack bifurcation in the compressive layers under bending

For a laminate subjected to flexural loading, where the load is applied normal to the layer plane, a crack propagating perpendicularly to the layers is prone to bifurcate in the compressive layer if $t\sigma_R^2$ is larger than a critical value. If the compressive residual stress $\sigma_R$ is given, a critical layer thickness exists, above which crack bifurcation will occur [9]. The mechanism of crack bifurcation is similar to that of edge cracking: when a crack propagates into a compressive layer, the relaxation of the compressive residual stress on the crack surfaces creates a tensile stress perpendicular to the layer plane, which may cause the crack to deflect and bifurcate [9,11].

### 1.4. Relation between crack bifurcation and edge cracking

The phenomenon of crack bifurcation under four-point bending has been investigated with the load oriented either parallel [8,12–14] or normal to the layer plane [9–11,15]. In most of experimental studies it was found that crack bifurcation was preceded by edge cracking. As edge cracks have a detrimental effect on the structural integrity of laminate, it was suggested that crack bifurcation should be avoided in laminate design in order to prevent edge cracking. Recent experimental results show, however, that a crack could bifurcate in some laminates without edge cracks [13,15]. This means that special conditions may exist, under which edge cracking during the cooling process can be prevented while crack bifurcation during the bending still occurs.

For ceramic laminates with residual stresses, fracture strength and fracture toughness of the laminates can be easily predicted if the crack propagation is straight. However, modelling crack bifurcation in laminates is not easy [14,16]. The purpose of this paper is to understand the conditions for crack bifurcation and edge cracking in laminates. To do this, finite element (FE) calculations are performed to analyze edge cracking and crack bifurcation in two laminates.

## 2. Material and preliminary experimental investigations

### 2.1. Architecture and material properties of the laminates

The laminates were fabricated via sequential slip casting. The slurry composed of $Al_2O_3$/5 vol.% t-$ZrO_2$, referred to as ATZ, was used to form the thick layers. For the thin layers the slurry containing $Al_2O_3$/30 vol.% m-$ZrO_2$ was employed, referred to as AMZ. The m-$ZrO_2$ was used to promote high compressive residual stresses in AMZ layers [15]. Two laminates were designed. Each consisted of five thick ATZ layers alternated with four thin AMZ layers. The main difference between two laminates is the AMZ layer thickness. The material properties of layers were evaluated on monolithic ATZ and AMZ. Young's modulus $E$, Poisson's ratio $\nu$, and failure stress $\sigma_m^f$ are listed in Table 1. The $\sigma_m^f$ is the maximum of stress $\sigma_{xx}$ at the upper surface, caused by the applied load.

Due to the thermal misfit between ATZ and AMZ layers and due to the phase transformation in AMZ layers, residual stresses develop during the cooling from the sintering temperature. A total strain difference of $\Delta\varepsilon = -2.12 \times 10^{-3}$ exists between AMZ and ATZ layers, which was measured in previous works through dilatometer measurements on bulk ceramics with the same composition of the layers [15].

Although the compressive residual stresses are beneficial to fracture properties, the tensile residual stresses are harmful. To avoid high tensile residual stresses, the thickness ratio of the tensile layer to the compressive layer should be high enough. Table 2 collects the thicknesses $t_1$ and $t_2$ of ATZ and AMZ layers, the thickness ratios, the total thickness of each laminate, and the biaxial residual stress. The idea of using this kind of layered architectures is to increase strength reliability. If the crack bifurcation occurs in bending, the toughness will be increased. However, if edge cracking occurs, the structural integrity may be damaged.

If elastic mismatch is not considered, the critical thickness $t_c$ for a AMZ layer to prevent edge cracking can be estimated by Eq. (1), resulting in $t_c \approx 41.7$ μm for laminate B and $t_c \approx 38.6$ μm for laminate C. Rao and Lange [8] stated an experiment-based critical thickness for generating edge cracking, $2t_c$. For laminate B, since $t_2/t_c = 2.28 > 2.0$, we can predict that edge cracking will occur. For laminate C, since $t_2/t_c = 1.55 < 2.0$, we can predict that edge cracking will not occur if there is not a very large flaw at the edge surfaces of AMZ layers. Optical microscopy revealed edge cracks in laminate B and no edge crack in laminate C.

**Table 1**
Material properties of the layers forming the laminate.

| Material | $E$ (GPa) | $\nu$ (1) | $\sigma_m^{crit}$ (MPa) | $K_{Ic}$ (SEVNB) (MPa m$^{1/2}$) | $J_{Ic}$ (J/m$^2$) |
|---|---|---|---|---|---|
| ATZ | 390 ± 10 | 0.22 | 422 ± 30 | 3.2 ± 0.2 | 25 ± 1 |
| AMZ | 280 ± 30 | 0.22 | 90 ± 20 | 2.6 ± 0.2 | 23 ± 1 |

**Table 2**
Geometry and residual stresses of laminates B and C.

| Laminate | $t_1$ (μm) | $t_2$ (μm) | $t_1/t_2$ (1) | $t_{total}$ (μm) | $\sigma_1$ (MPa) | $\sigma_2$ (MPa) |
|---|---|---|---|---|---|---|
| B | 540 | 95 | 5.7 | 3080 | 97 | −691 |
| C | 570 | 60 | 9.5 | 3090 | 60 | −718 |

### 2.2. Flexural fracture tests

In each specimen, three indentation cracks were created on the upper surface, with an offset separation of 2 mm to avoid crack interaction. The indented specimens were fractured under four-point bending with the loading axis normal to the layer plane. Fig. 2 shows the stress $\sigma_m$ vs. cross-head displacement curves for laminate B, laminate C and ATZ monolith (curve A). $\sigma_m$ is the stress $\sigma_{xx}$ at the upper surface of specimen, caused by the applied load. In ATZ monolith, failure occurred at $\sigma_m^f$ = 140 MPa. Laminates B and C showed a stepwise fracture. The final failure stress (threshold strength) was $\sigma_m^f$ = 160 MPa for laminate B and 195 MPa for laminate C. In both laminates, bifurcation took place. The bifurcated crack path was longer in laminate B than in laminate C. In both laminates the bifurcation initiated after the crack tip had entered the compressive layer for a small distance. The deflection angle of the bifurcated cracks was 70–75° to the initial crack path.

## 3. Models

The 2D FE models with eight-node plane strain elements are designed. ABAQUS is employed for computations. The misfit strain between AMZ and ATZ at room temperature is $-2.12 \times 10^{-3}$. The material properties at room temperature are defined as:

ATZ: $E$ = 390 GPa, $v$ = 0.22, $K_{Ic}$ = 3.2 MPa m$^{1/2}$, $J_{Ic}$ = 25.0 J/m$^2$;
AMZ: $E$ = 280 GPa, $v$ = 0.22, $K_{Ic}$ = 2.6 MPa m$^{1/2}$, $J_{Ic}$ = 23.0 J/m$^2$.

Where, the critical $J$-integrals are transformed from $K_{Ic}$ by

$$J_{Ic} = K_{Ic}^2(1 - v^2)/E. \tag{2}$$

### 3.1. FE model for edge cracking

We use a three-layer ATZ/AMZ/ATZ-laminate to replace the nine-layer laminate. The AMZ layer thickness and the AMZ volume fraction in the three-layer laminate are defined identical to the nine-layer laminate, so the residual stresses in

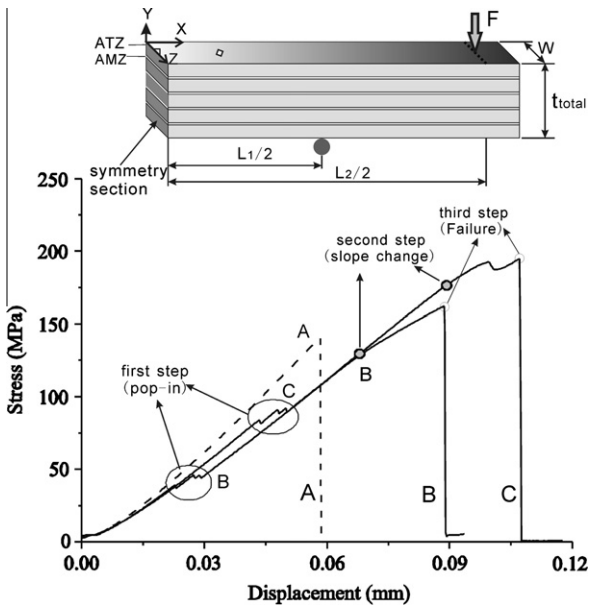


**Fig. 2.** Stress $\sigma_m$ vs. cross-head displacement curves of laminate B, laminate C and ATZ monolith (curve A) under four-point bend. Half of the specimens is shown, with $t_{total} \approx$ 3.1 mm, $W$ = 3.6 mm, $L_1$ = 15 mm and $L_2$ = 30 mm.

the three-layer laminate are the same as in the nine-layer laminate. One-fourth of the cross-section in $z$–$y$ plane of the three-layer laminate is used as FE model. The bottom boundary of the model is the mid-plane of the AMZ layer. We apply a unit temperature drop and assume the thermal expansion coefficients to be 0 and $-2.12 \times 10^{-3}$ for ATZ and AMZ, respectively, to generate residual stresses. Edge cracking is simulated by releasing the corresponding nodes at the bottom boundary.

To calculate the elastic strain energy release rate $G_{ED}$ for the crack propagation in $z$-direction (edging), it is assumed that the crack is very long in $x$-direction so that the plane strain model can be applied. $G_{ED}$ equals the near-tip $J$-integral. The elastic strain energy release rate $G_{CH}$ for the crack propagation in $x$-direction (channelling) cannot be directly calculated by a plane strain model, since channelling is a three-dimensional problem. However, if the surface crack length is much larger than the crack depth, $G_{CH}$ will be independent of the crack length, and can be obtained from $G_{ED}$ [5]

$$G_{CH} = \frac{1}{a}\int_0^a G_{ED}\,da, \tag{3}$$

where $a$ denotes the crack depth.

### 3.2. A method for analyzing the early stage of edge cracking

For a compressive thin layer sandwiched between two very thick layers, along the mid-plane ($y = 0$) of the compressive layer, the residual stress near the edge surface is

$$\sigma_{yy,res}(z)/|\sigma_R| = \frac{2}{\pi}\left(\theta - \frac{1}{2}\sin 2\theta\right), \tag{4}$$

where $\tan\theta = \frac{t_2}{2z}$; $z$ is the distance away from the edge surface, and $t_2$ the compressive layer thickness [5]. At the mid-plane $y = 0$, Eq. (4) for $0 \leqslant z \leqslant a$ can be expressed as

$$\sigma_{yy,res}(z)/|\sigma_R| \approx A_0 + A_1\xi + A_2\xi^2 + A_3\xi^3, \tag{5}$$

where $\xi = 1 - \frac{z}{a}$. Table 3 shows the values of $A_i$ in Eq. (5) for different $a/t_2$ values. For a semi-elliptical surface crack, the stress intensity factor can be calculated by Murakami [17]

$$K_I = \frac{|\sigma_R|\sqrt{\pi a}}{\Phi}\sum A_i M_i \quad i = 0, 1, 2, 3. \tag{6}$$

$\Phi$ denotes the complete elliptical integral of the second kind. For $a_L/a \geqslant 1$,

$$\Phi = \int_0^{\frac{\pi}{2}} (1 - r^2\sin^2\varphi)^{\frac{1}{2}} d\varphi, \tag{7}$$

where $r = \left(1 - \frac{a^2}{a_L^2}\right)^{\frac{1}{2}}$. Here, $a$ is the crack depth, and $a_L$ the half length of the semi-elliptical crack. Table 4 shows the values of $M_i$ for $a_L/a = 1.0$, 1.667 and 2.5 [17]. As $G = K_I^2/E'$, where $E' = E/(1 - \nu^2)$, the elastic energy release rate $G$ can be expressed as

$$\frac{E'G}{\sigma_R^2 t_2} = \frac{\pi}{\Phi^2}\frac{a}{t_2}\left(\sum A_i M_i\right)^2. \tag{8}$$

### 3.3. FE model for analysing straight crack propagation

Due to symmetry, only the right half of the nine-layer specimen in $x$–$y$ plane is analysed (see Fig. 2). First, the symmetry conditions are applied to the left boundary and a temperature change $\Delta T = -1$ is applied to the model to generate residual stresses. Second, the nodes behind the crack tip are released to create a crack at the left boundary. Third, a moment load is applied to the right boundary. The right boundary is constrained to be a straight line.

**Table 3**
Values of $A_i$ in Eq. (5) for different $a/t_2$ values.

| $a/t_2$ | $A_0$ | $A_1$ | $A_2$ | $A_3$ |
|---|---|---|---|---|
| 0.05 | 0.8735 | 0.1253 | 0.0013 | 0 |
| 0.10 | 0.7517 | 0.2388 | 0.0098 | 0 |
| 0.15 | 0.6385 | 0.3310 | 0.0312 | 0 |
| 0.20 | 0.5368 | 0.3958 | 0.0691 | 0 |
| 0.30 | 0.3759 | 0.4367 | 0.1948 | 0 |
| 0.40 | 0.2588 | 0.3755 | 0.3716 | 0 |
| 0.50 | 0.1854 | 0.2476 | 0.5720 | 0 |
| 0.60 | 0.1336 | 0.1794 | 0.5407 | 0.1544 |
| 0.70 | 0.0979 | 0.1421 | 0.3973 | 0.3756 |

**Table 4**
Values of $M_i$ in Eq. (6) for points A and C.

| $a_L/a$ | Position | $M_0$ | $M_1$ | $M_2$ | $M_3$ |
|---|---|---|---|---|---|
| 1.0 | A | 1.039 | 0.299 | 0.166 | 0.114 |
| 1.0 | C | 1.133 | 0.951 | 0.836 | 0.751 |
| 1.667 | A | 1.069 | 0.371 | 0.216 | 0.151 |
| 1.667 | C | 0.933 | 0.779 | 0.678 | 0.605 |
| 2.5 | A | 1.087 | 0.418 | 0.252 | 0.179 |
| 2.5 | C | 0.794 | 0.666 | 0.581 | 0.519 |

### 3.4. Model for analysing the bifurcated cracks

The model for analysing the bifurcated cracks is similar to that for a straight crack. The main difference is that a branch crack exists with an angle $\varphi = 70°$ to the straight (0°) crack path. The calculation steps are the same as those for the straight crack.

## 4. Results and discussion

### 4.1. Comparison of energy release rates between two laminates when the length of an edge crack is much larger than the crack depth

Fig. 3 shows the variation of $G_{ED}$ as a function of $a$ for the cracks propagating in $z$-direction (edging), where $a$ denotes the edge crack size in $z$-direction, and $G_{ED}$ is identical to the near-tip $J$-integral. For $a < 6$ μm, $G_{ED}$ of laminate C is similar to that of laminate B. With the increase of $a$, the $G_{ED}$ of laminate C becomes lower than that of laminate B. If edge cracking occurs, the equilibrium crack depth will be $a = 130$ μm for laminate B and $a = 43$ μm for laminate C. Fig. 3 also shows the variation of the elastic energy release rate $G_{CH}$ for crack channelling (in $x$-direction) as a function of $a$. The $G_{CH}$ was calculated from Eq. (3) using $G_{ED}$ values. For $a < 9$ μm, $G_{CH}$ of laminate C is similar to that of laminate B. With the increase of $a$, the $G_{CH}$ of laminate C becomes distinctly lower than that of laminate B. For both laminates, $G_{ED} = J_{Ic}$ occurs at $a \approx 4$ μm and $G_{CH} = J_{Ic}$ at $a \approx 9$ μm. Edge cracking can be prevented if the $z$-direction size of a surface crack is smaller than 4 μm.

### 4.2. Comparison of energy release rates between two laminates when a semi-elliptical crack exists at an edge surface

By using Eq. (8), energy release rates are calculated for a semi-elliptical surface crack, shown as Fig. 4, where $G_A$ and $G_C$ are elastic energy release rates at points A and C, respectively. If the initial crack has a semi-circular shape, then in both laminates B and C the crack cannot propagate in $z$-direction, independent of its initial size, since $G_A < J_{Ic}$ for all values of $a/t_2$. However, the semi-circular crack can grow in $x$-direction if $a$ is large enough. For laminate B, $G_C = J_{Ic}$ occurs at $a/t_2 = 0.10$, i.e., at $a = 9.5$ μm. If $a < 9.5$ μm, the semi-circular crack at the edge surface of laminate B cannot propagate. For laminate C, $G_C = J_{Ic}$

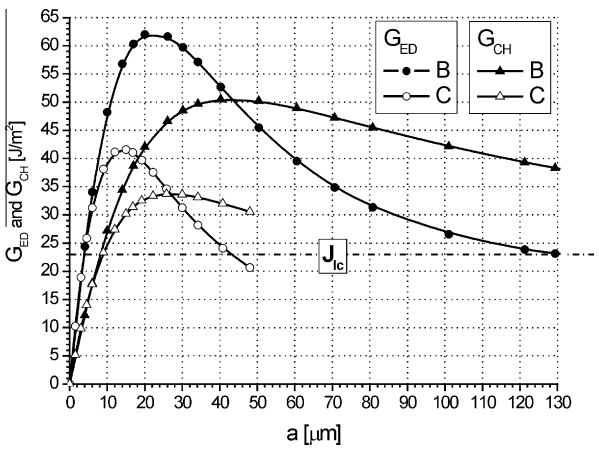


**Fig. 3.** Variations of $G_{ED}$ and $G_{CH}$ with $a$ when the length of edge crack is much larger than crack depth. $G_{ED}$ and $G_{CH}$ represent elastic strain energy release rates for crack propagations in $z$-direction (edging) and $x$-direction (channelling), respectively; $a$ is the crack depth in $z$-direction; $J_{Ic}$ is the critical $J$-integral of AMZ layer.

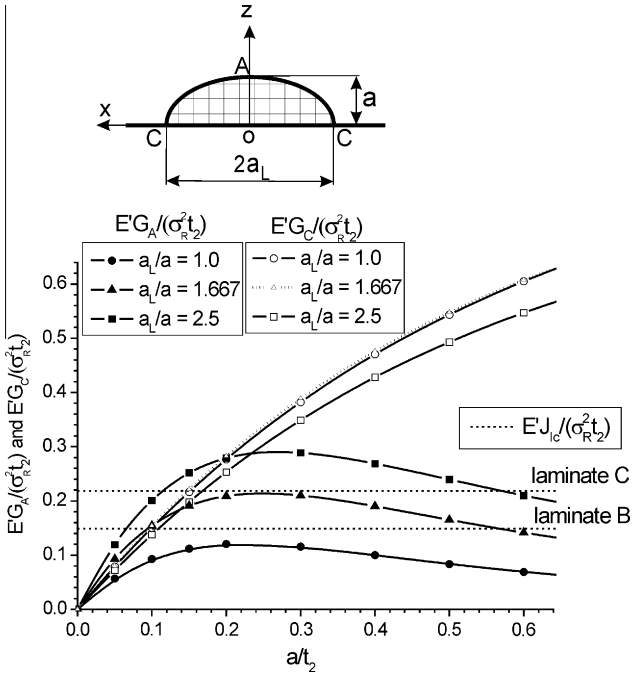


**Fig. 4.** Elastic strain energy release rates of a semi-elliptical crack at the edge surface of a compressive layer. $G_A$ and $G_C$ are energy release rates at points A and C, respectively.

occurs at $a/t_2 = 0.15$, i.e., at $a = 9.0$ μm. If $a < 9.0$ μm, the semi-circular crack at the edge surface of laminate C cannot propagate. If the initial surface crack has a semi-elliptical shape with $a_L/a = 2.5$, then $G_A$ will be higher than $G_C$ when $a/t_2 < 0.24$, and whether the crack can propagate will depend on $G_A$. For laminate B, $G_A = J_{Ic}$ occurs at $a/t_2 = 0.065$, i.e., at $a = 6.2$ μm. For laminate C, $G_A = J_{Ic}$ occurs at $a/t_2 = 0.115$, i.e., at $a = 6.9$ μm.

From the numerical results it is known that the critical size of the initial crack for preventing edge cracking is similar for laminates B and C, because the residual stress $\sigma_{yy,res}$ near the edge surface is similar in both laminates when $z$ is small. Then,

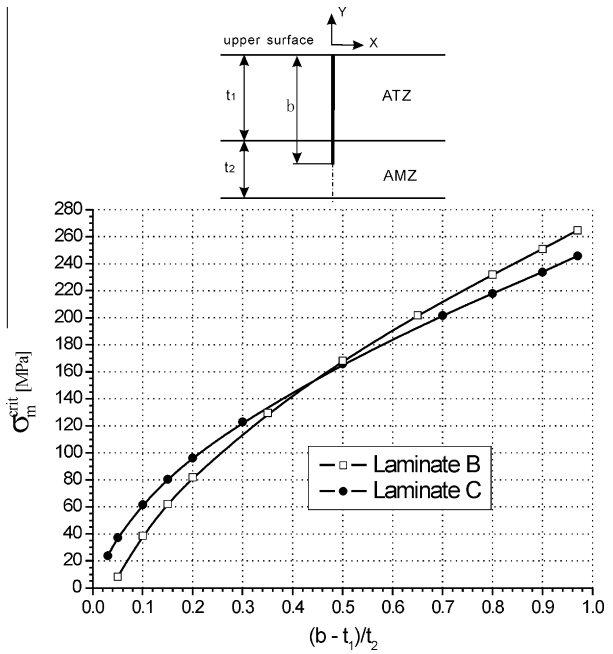


**Fig. 5.** Comparison of $\sigma_m^{crit}$ vs. $(b - t_1)/t_2$ curves between laminates B and C. $\sigma_m^{crit}$ is the critical applied stress, and $b$ the crack length.

why laminate B has edge cracks while laminate C has no edge crack? It might be due to the fact that the possibility of large flaws existing near the edge surfaces of laminate B is higher than laminate C. This is because, (1) the edge surface of the compressive layer thickness is about 60% larger in laminate B than in laminate C; (2) the tensile residual stress region near the edge surface of compressive layer is about 60% deeper in laminate B than in laminate C.

### 4.3. Propagation of a straight crack normal to the layer plane

To understand the effects of crack bifurcation on the fracture strength and toughness of a laminate, it is necessary to know how the load varies with the crack extension if the crack propagation were straight.

The geometrical difference between laminates B and C is the thickness of the compressive AMZ layer: the AMZ layer thickness $t_2$ in laminate B is about 60% higher than that in laminate C, while the ATZ layer thickness $t_1$ in laminate B is similar to that in laminate C. The residual stress difference between laminates B and C is the tensile residual stress $\sigma_1$ of ATZ layer: the tensile stress $\sigma_1$ in laminate B is about 60% higher that that in laminate C, while the compressive stress $\sigma_2$ of AMZ layer is only a few percent lower in laminate B than in laminate C. As a result, $\sigma_2 t_2$ and $\sigma_1 t_1$ in laminate B are about 52% larger than those in laminate C. When the crack tip is located near the second interface, the shielding effect of compressive residual stress $\sigma_2$ of AMZ layer in laminate B is higher than in laminate C, while the anti-shielding effect of tensile residual stress $\sigma_1$ of ATZ layer in laminate B is also higher than in laminate C.

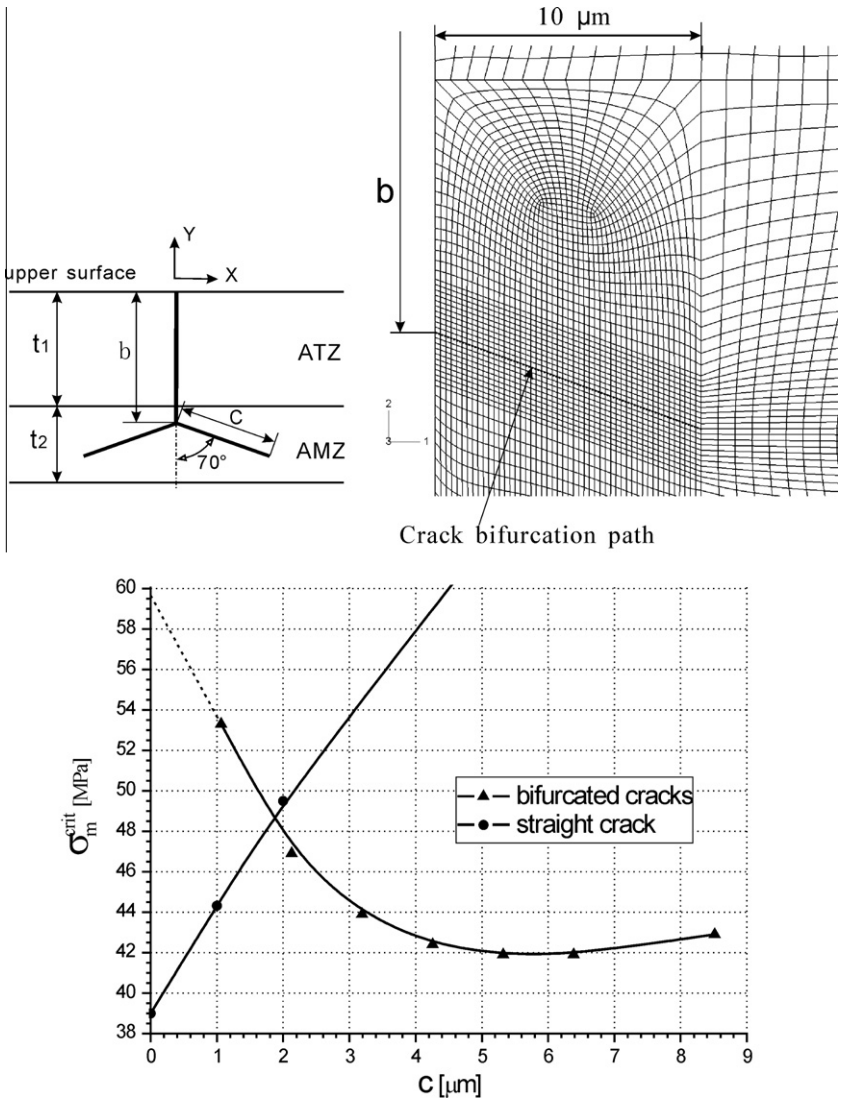


**Fig. 6.** Comparison of $\sigma_m^{crit}$ vs. $c$ curves between bifurcated and straight cracks inside the first AMZ layer of laminate B. $c$ is the crack extension from the bifurcation point.

Fig. 5 shows the variation of the critical applied stress $\sigma_m^{crit}$ that makes $J_{tip} = J_{Ic}$. If $(b - t_1)/t_2 < 0.45$, the load of laminate C is higher than laminate B; if $(b - t_1)/t_2 > 0.45$, the load of laminate C becomes lower than laminate B. The load corresponding to $(b - t_1)/t_2 \to 1.0$, i.e., the threshold strength, is 270 MPa for laminate B and 250 MPa for laminate C. Therefore, if the crack path were straight, the threshold strength of laminate B would be higher than that of laminate C. Experimental results (Fig. 2) reveal that the measured threshold strength of laminate B is lower than that of laminate C. Also, the experimentally measured threshold strengths of both laminates are lower than those predicted in Fig. 5. Therefore, crack bifurcation will reduce the threshold strength. FE results support a viewpoint obtained from experiment [15]: If the bending load is normal to the layer plane, crack bifurcation will increase the toughness and decrease the threshold strength.

### 4.4. Near-tip J-integral at the initiation of crack bifurcation

A question is, under what conditions the $J$-integral in the direction of the bifurcated crack can reach $J_{Ic}$ earlier than the $J$-integral in the straight crack direction. To answer this question, laminate B is analyzed. We assume that the straight crack has entered the compressive layer for 10% of the layer thickness, i.e., $b - t_1 = 9.5$ μm, which was near the bifurcation point detected in the experiment. The bifurcation directions are assumed to be 70° to the straight crack direction, as found in the experiment. The $J$-integral in the direction of the bifurcated crack at the initiation of crack bifurcation cannot be directly calculated at the tip of the existing straight crack. To estimate this value, the near-tip $J$-integral around the tip of a bifurcated crack is calculated for a series of crack extension $c$ in the direction of 70° to the initial crack. In the FE model for calculating crack bifurcation, eight-node plane strain element is applied. There are about 30,000 nodes and about 10,000 elements. The local mesh near a bifurcated crack branch is shown in Fig. 6. The crack bifurcation is realized by separating the nodes along the bifurcation path.

Fig. 6 compares the $\sigma_m^{crit}$–$c$ curves between a straight crack and a bifurcated crack. The critical applied stress $\sigma_m^{crit}$ is obtained by setting $J_{tip} = J_{Ic}$. For the bifurcated crack extension, $\sigma_m^{crit}$ decreases rapidly with the increase of $c$, provided that $c$ is smaller than 5 μm; while for the straight crack extension, $\sigma_m^{crit}$ increases rapidly with the increase of $c$. This means crack bifurcation is unstable while straight crack propagation is stable. If $c > 1.8$ μm, the $\sigma_m^{crit}$ of a bifurcated crack will be lower than that of the straight crack, which means that crack bifurcation can occur at $b - t_1 = 9.5$ μm if micro-cracks are so large that the effective crack length is increased by 1.8 μm. Therefore, if micro-cracks around crack tip are taken into account, the near-tip $J$-integral can explain the crack bifurcation.

## 5. Conclusions

Experimental results show that when the compressive layer thickness was $1.55t_c$, edge cracking did not occur, where $t_c$ is the critical thickness for avoiding edge cracking. This means that the critical thickness for generating edge cracking is significantly higher than $t_c$.

If the flexural load is normal to interfaces, crack bifurcation increases the toughness of laminate, but decreases the threshold strength of laminate.

By using a simple method, the critical size for a semi-elliptical surface crack can be determined, below which the pre-existing cracks at edge surfaces cannot propagate.

The initiation of crack bifurcation in ceramic laminate can be explained by the near-tip $J$-integral, provided that micro-cracks exist around the crack tip.

## Acknowledgements

R. Bermejo thanks Dr. Sanchez-Herencia for providing the materials. O. Kolednik acknowledges partial support by the Comet K2 Competence Centre in Leoben, Austria. C.R. Chen thanks Professor Y.W. Mai and Australian Research Council (ARC) for supporting this work with the project DP#0665856.

## References

[1] He MY, Hutchinson JW. Crack deflection at an interface between dissimilar elastic materials. Int J Solids Struct 1989;25:1053–67.
[2] Phillipps AJ, Clegg WJ, Clyne TW. Fracture behavior of ceramic laminates in bending-I. Modeling of crack-propagation. Acta Metal Mater 1993;41:805–17.
[3] Sanchez-Herencia AJ, James L, Lange FF. Bifurcation in alumina plates produced by a phase transformation in central, alumina/zirconia thin layers. J Eur Ceram Soc 2000;20:1297–300.
[4] Bermejo R, Pascual J, Lube T, Danzer R. Optimal strength and toughness of $Al_2O_3/ZrO_2$ laminates designed with external or internal compressive layers. J Eur Ceram Soc 2008;28:1575–83.
[5] Ho S, Hillman C, Lange FF, Suo Z. Surface cracking in layers under biaxial residual compressive stress. J Am Ceram Soc 1995;78:2353–9.
[6] He MY, Evans AG. Criterion for the avoidance of edge cracking in layered system. J Am Ceram Soc 2004;87:1418–23.
[7] Monkowski AJ, Beltz GE. Suppression of edge cracking in layered ceramic composites by edge coating. Int J Solids Struct 2005;42:581–90.
[8] Rao MP, Lange FF. Factors affecting threshold strength in laminar ceramics containing thin compressive layers. J Am Ceram Soc 2002;85:1222–8.
[9] Oechsner M, Hillman C, Lange FF. Crack bifurcation in laminar ceramic composites. J Am Ceram Soc 1996;79:1834–8.
[10] Sanchez-Herencia AJ, Pascual C, He J, Lange FF. $ZrO_2/ZrO_2$ layered composites for crack bifurcation. J Am Ceram Soc 1999;82:1512–8.
[11] Lugovy M, Orlovskaya N, Slyunyayev V, Gogotsi G, Kubler J, Sanchez-Herencia AJ. Crack bifurcation features in laminar specimens with fixed total thickness. Compos Sci Technol 2002;62:819–30.

[12] Rao MP, Sanchez-Herencia AJ, Beltz GE, McMeeking RM, Lange FF. Laminar ceramics that exhibit a threshold strength. Science 1999;286:102–5.
[13] Pontin MG, Lange FF. Crack bifurcation at the surface of laminar ceramics that exhibit a threshold strength. J Am Ceram Soc 2005;88:1315–7.
[14] Hbaieb K, McMeeking RM, Lange FF. Crack bifurcation in laminar ceramics having large compressive stress. Int J Solids Struct 2007;44:3328–43.
[15] Bermejo R, Torres Y, Sanchez-Herencia AJ, Baudin C, Anglada M, Llanes L. Residual stresses, strength and toughness of laminates with different layer thickness ratios. Acta Mater 2006;54:4745–57.
[16] Bahr HA, Pham VB, Weiss HJ, Bahr U, Streubig M, Balke H, et al. Threshold strength prediction for laminar ceramics from bifurcated crack path simulation. Int J Mater Res 2007;98:683–91.
[17] Murakami Y, editor. Stress intensity factors handbook. 3rd ed. vol. 3. New York: ASME Press; 2000.